A single step assembly of carbon nanotube fabric containing embedded copper particles produced from advanced electrolytic baths

Neta Yitzhack,[1] and Yair Ein-Eli[z,1,2,3]

[1] Department of Materials Science and Engineering, Technion – Israel Institute of Technology, Haifa 3200003, Israel

[2] The Nancy & Stephan Grand Technion Energy Program (GTEP), Technion – Israel Institute of Technology, Haifa 3200003, Israel

[3] Institut für Energie- und Klimaforschung (IEK-9: Grundlagen der Elektrochemie), Forschungszentrum Jülich, D-52425 Jülich, Germany

[z]Corresponding Author's E-mail Address: eineli@technion.ac.il

Abstract

The electrodeposition of copper particles inside carbon nanotube (CNT) tissues is presented here. Copper electrodeposition inside CNT from aqueous electrolytes has been challenging researchers in recent years, as deposition was mostly restricted to the external surface of the tissue. This work introduces several organic additives, promoting deposition inside the tissue, as well. Electrochemical methods were applied and utilized in order to study the behavior of the CNT in the plating bath, and to analyze the effect of different additives on the deposition of the copper particles. Surface morphology of the coating and the deposits inside the tissue were examined and studies. This work presents an alternative method for the deposition and implementation of copper crystals inside CNT tissue.

1.0 Introduction

The increasing demand for electrical energy stimulates research to consider alternative materials for the common copper (Cu) wires, widely used nowadays. This search for innovative electrically conducting materials is focused, among others, on achieving maximum current carrying capacities (ampacity), increasing the designed electrical material conductivity per weight, as well as enhancing the mechanical properties, such as strength and flexibility.

One intriguing material, in this context, is a composite material combining carbon nanotube (CNT) and Cu. In the last decade, the synthesis of this material has been challenging the scientific community. Electrodeposition of Cu offers a rather simple preparation method for this composite material. Copper electroplating is a widely studied field; many methods for Cu electroplating have been developed, modified and adjusted to the numerous requirements different applications might have. These methods are already employed in the industry; however, attempts to apply them for a deposition inside the CNT tissue were found to be inefficient, as copper was plated exclusively on the external surface of the CNT tissue.[1–3] One method developed so far, involves the electrodeposition of Cu in a two-step process.[4–9] First, Cu is deposited from an organic electrolyte containing copper acetate [$Cu(OAc)_2$] in anhydrous acetonitrile (MeCN), enabling optimal seeding of Cu within the CNT.[5,7] The sample is than annealed under hydrogen flow, followed by a second electrodeposition of Cu from an aqueous $CuSO_4$ electrolyte enabling the growth of Cu seeds. Nevertheless, this process is tedious and resource-consuming; especially, since the organic electrodeposition step results in an extremely low faradaic efficiency.[5] Thus, a simpler and more efficient technique is of interest. This paper presents such a process, where Cu is deposited inside the CNT tissue in a one-step electrodeposition process, carried out in an aqueous copper sulfate electrolyte. Several organic additives to the electrolyte are studied and shown to facilitate the electrodeposition of Cu inside CNT tissue.

2.0 Experimental

2.1. Electrolyte preparation: Two electrolytes were prepared with different concentrations of copper sulfate ($CuSO_4$), and sulfuric acid (H_2SO_4); the first one with high concentration of copper ions, used in conventional acidic $CuSO_4$ baths (denoted in **Table 1** as I), and the second with lower copper content, conventional to acidic $CuSO_4$ baths with relatively high throwing power (denoted in **Table 1** as II).[10] Polyethylene glycol (PEG, 2,000 gr/mol), benzotriazole (BTAH), and acetonitrile (MeCN) were used as additives. Table 1 lists the exact compositions of the 5 electrolytes studied in this work.

Table 1. Composition of $CuSO_4$ electrolytes.

	I	II	II+PEG	II+BTAH	II+MeCN
$CuSO_4 \cdot 5H_2O$ [gr/L]	200	59	59	59	59
H_2SO_4 [gr/L]	45	210	210	210	210
Cl^- [ppm]	-	30	30	30	30
PEG [ppm]	-	-	500	-	-
BTAH [mM]	-	-	-	0.1	-
MeCN [ppm]	-	-	-	-	1000

2.2. Electrochemical cell: Electrochemical measurements were performed in a three-electrode cell, employing a standard calomel electrode (SCE) as a reference electrode; copper (Cu) foil (99.99%) as a counter electrode; and carbon nanotube (CNT) tissues (Tortech nanofibers (Israel), 0.75 mg/cm^2) as a working electrode (1x1 cm^2, 20 μm thick).

The CNT tissue used in the experiments is composed of randomly oriented multi-wall CNT (MWCNT), and was used as received without further modification. An HR-SEM image obtained from the pristine tissue is presented in **Figure S1**. This micrograph displays the morphology and porous structure of the tissue. Based on it, the estimated nanotube diameter is 30±9 nm. Raman spectrum of the tissue was recorded with XploRA Raman spectrometer (Horiba Scientific), equipped with a 532 nm laser, and is presented in **Figure S2**.

2.3. Electrochemical Studies: cyclic voltammograms were obtained at a sweep rate of 20 mV/sec, starting from an open circuit potential (OCP), scanning toward cathodic potentials until the first vertex potential (-0.3 V_{SCE}), then shifting the direction of the scan until a second vertex potential (0.4 V_{SCE}) is reached, and back to OCP. Copper was deposited on CNT tissue electrodes under galvanostatic conditions, applying -10 mA/cm^2 for 15 min., allowing satisfying number of deposits for further examination, based on preliminary comparison among several deposition conditions (**Figure S3**). The samples were thoroughly rinsed in deionized water to remove excess electrolyte.

2.4. Deposits characterization: surface morphology was imaged with a high-resolution scanning electron microscope (HR-SEM, Zeiss, Ultra-Plus), using both a secondary electron (SE) detector and an energy selective backscattered (ESB) electron detector. Images were obtained from the upper coating layer, as well as from inside of the CNT tissue. CNT tissue samples for imaging the inside layers were prepared by peeling off the upper Cu coating, thus exposing an inner layer of the tissue. The chemical composition of the deposits was determined by energy dispersive x-ray spectroscopy (EDS), and by X-ray diffraction (XRD) carried out in an X-ray diffractometer equipped with a Cu target (Rigaku, MiniFlex).

3.0 Results and Discussion

3.1. Additive-free electrolytes

Two compositions of additive-free electrolytes were prepared as detailed in Table 1: the standard electrolyte contains high concentration of Cu, and it is the conventional composition used for industrial Cu electroplating. The other electrolyte contains a low Cu concentration and is more acidic. This electrolyte is characterized with higher throwing-power[10] and is also commonly used in Cu electroplating processes for specific applications.

The electrolyte uptake by a CNT tissue in the high Cu ion content electrolyte was measured over a period of 24 hr and compared to the electrolyte uptake of an organic electrolyte based on MeCN. The electrolyte uptake of the aqueous electrolyte was about 100 times higher than that of the organic electrolyte (**Figure S4**). Thus, it is evident that a CNT tissue can, to some extent, absorb the aqueous $CuSO_4$ electrolyte, suggesting that the hydrophobic nature of the tissue may not be a limiting factor in the electrodeposition of Cu inside it. It should be noted that the aqueous electrolyte is very acidic (pH=0.5), due to the high concentration of sulfuric acid; this in-turn improves its interaction with the CNT and contributes to higher electrolyte uptake.[11] Further studies involving various compositions of the aqueous $CuSO_4$ electrolyte were conducted and are presented hereinafter.

3.1.1. Additive-free electrolytes- Electrochemical studies

Cyclic voltammograms (presented in Figure 1) were recorded, and three consecutive sweeps were collected. For comparison, cyclic voltammograms were also recorded on a Pt working electrode, as well as on a CNT electrode in an electrolyte containing no dissolved copper ions while employing a Pt counter electrode.

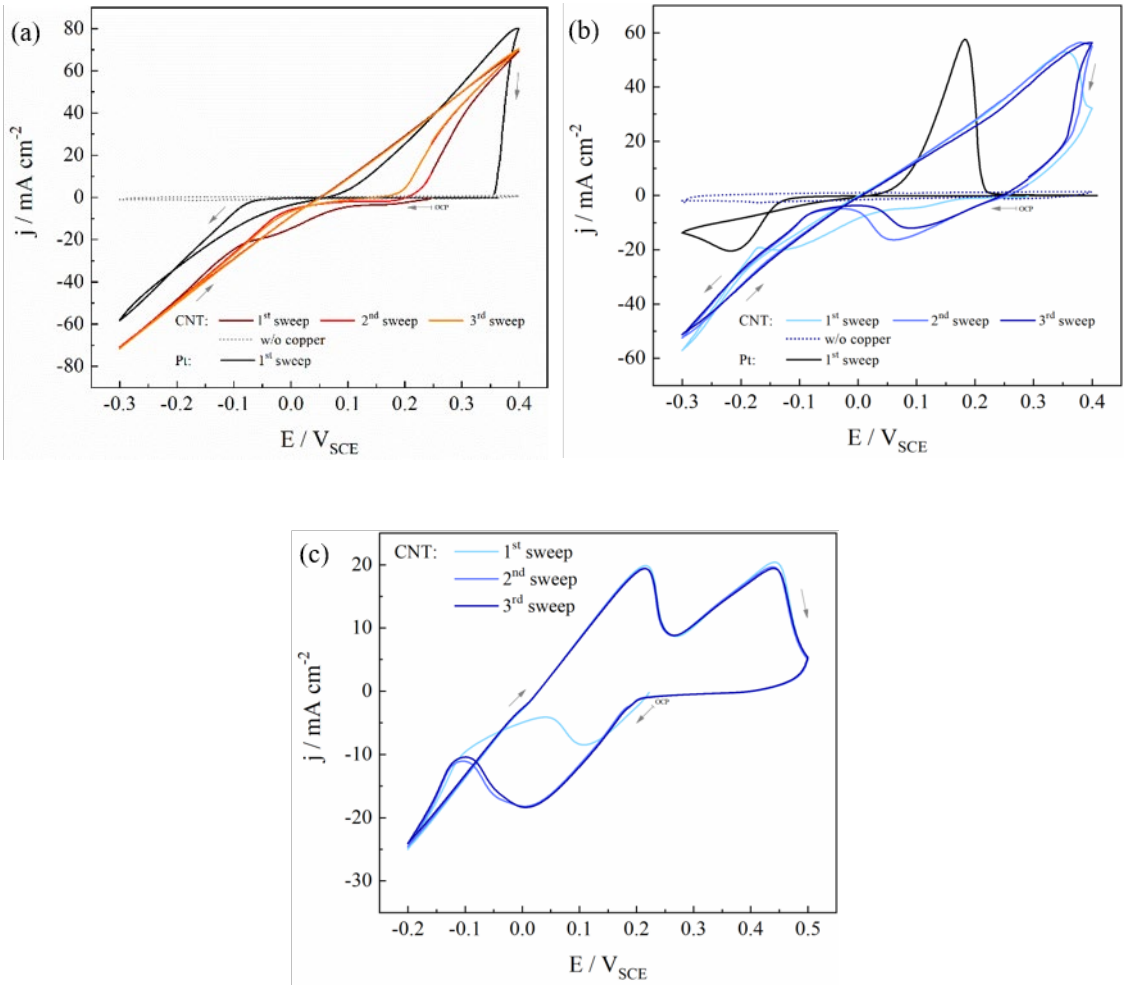

Figure 1: Cyclic polarization curves recorded with CNT working electrodes from additive-free $CuSO_4$ electrolytes: (a) high-Cu ion content in the electrolyte; (b), (c) low-Cu ion content in the electrolyte.

An increase in the cathodic currents on a CNT electrode is recorded in the electrolyte containing high Cu concentration (Figure 1a), immediately after applying the cathodic polarization and becomes more significant at potentials below 0.1 V_{SCE}. Further increase in the recorded current can be observed under potentials of ca. -0.06 V_{SCE}, both on CNT and Pt electrodes. This current increase is associated with Cu nucleation overpotential.[12] Upon repeating CV cycles, the first cathodic peak observed on the CNT electrode disappears, and the

curve becomes similar to the one being obtained and recorded while Pt was utilized as the working electrode. The overpotential for copper nucleation, is however lower from the 2nd sweep on, and stands on ca. 0.05 V_{SCE}. The anodic branch of the curve indicates a stripping process and an electrochemical dissolution of the deposited copper, upon exposure to the anodic potentials. Due to the irreversible hydrogen evolution reaction under higher cathodic potentials, occurring simultaneously with the reduction of Cu ions, the coulombic efficiency of each cycle is lower than 100%. Therefore, Cu dissolution's efficiency cannot be determined based on this value. Thus, it is possible that at the end of the first sweep, residues of metallic Cu on the electrode surface are present due to incomplete copper dissolution, shifting the cathodic onset potential during the consecutive sweeps. However, after reaching the second vertex potential, the scan direction was reversed, and the anodic currents decreased. Unlike the currents measured during the direct scan, the currents measured during the reverse scan were negligible, within the potentials range of ca. 0.2 and 0.05 V_{SCE}. This indicates a complete dissolution of the deposited copper during the initial part of the scan, when cathodic potentials were applied.

A comparison can be made to the voltammograms recorded in the electrolyte containing a lower Cu concentration (Figure 1b). In this case, an increase in the cathodic currents is observed under an onset potential of ca. 0.17 V_{SCE}. An additional rise of the current occurs under an onset potential of ca. -0.18 V_{SCE}. Again, the second cathodic peak is associated with Cu nucleation and deposition, and is observed on a Pt working electrode, as well. In this electrolyte, the deposition of copper is initiated at enlarged cathodic overpotentials, due to the lower concentration of copper ions in the electrolyte. Upon repeated cycles, the first cathodic peak is further increased and seems to reach a diffusion limited current. The overpotential for Cu nucleation decreases after the first sweep, and stands on ca. -0.08 V_{SCE}, which is lower than the potential recorded once Pt was utilized as the working electrode (ca. -0.13 V_{SCE}). The

voltammogram recorded for a CNT tissue electrode in a blank electrolyte, containing no dissolved copper ions, shows no significant reactions under this range of potentials. Thus, the first cathodic peak cannot be associated with any side reaction elated to a decomposition of the solvent, nor to surface reactions involving the CNT alone, but possibly may be attributed to present of copper species, present in the electrolyte.

Additional voltammograms were recorded and obtained from polarizing a CNT electrode in the electrolyte containing a low Cu ions concentration, under a narrower cathodic potential range (Figure 1c). In this case, the cathodic vertex potential was lower (-0.2 V_{SCE}), restricting the amount of deposited copper metal. This way, the anodic peak, observed as a single peak in the prior voltammograms, can be resolved into set of two peaks. This indicates that the additional cathodic reaction observed only while utilizing CNT electrodes is reversible, as well. The first cathodic reaction could be correlated to the reduction of Cu^{II} to Cu^{I}, which usually takes place under lower cathodic potentials than the reduction of Cu^{II} to Cu^{0}. Mono-valent Cu^{+} ions are much less stable than Cu^{2+} in acidic $CuSO_4$ solutions, and therefore the deposition of Cu is usually characterized by a single-step two-electron reaction. Nevertheless, the voltammograms recorded here suggest that perhaps in electrolytes containing low Cu ions concentrations, or in the presence of chloride ions, which is the only other difference between the two electrolytes, the CNT electrode stabilizes the Cu^{I}/Cu^{II} redox couple, converting the reduction into a two-step single-electron reaction.[13]

3.1.2. Additive-free electrolytes- Morphological studies

Metallic Cu was deposited on CNT electrodes from both electrolytes. HR-SEM images presented in **Figure 2** were obtained from the CNT external surface coating, as well as from the core deposits (inside the CNT tissue). From a comparison of the outer coating morphology

(Figure 2 (a, b)), it is confirmed that coarser deposits and increased surface roughness are obtained using the electrolyte containing a high Cu ion concentration, as could be expected, due to its lower throwing power. It appears that the different reduction mechanism of copper species observed on CNT electrodes (Figure 1) has no significant contribution to the deposition of Cu inside the CNT tissue.

HR-SEM images also validate that this electrolyte barely supports deposition of metallic Cu inside the tissue; only a few sporadic particles of metallic Cu can be observed inside the samples (as shown in Figure 2 (c, d)). The electrolyte with a low Cu ion concentration improves the metallic Cu deposition within the CNT tissue to some extent; yet, it is still depressed, and not homogeneous.

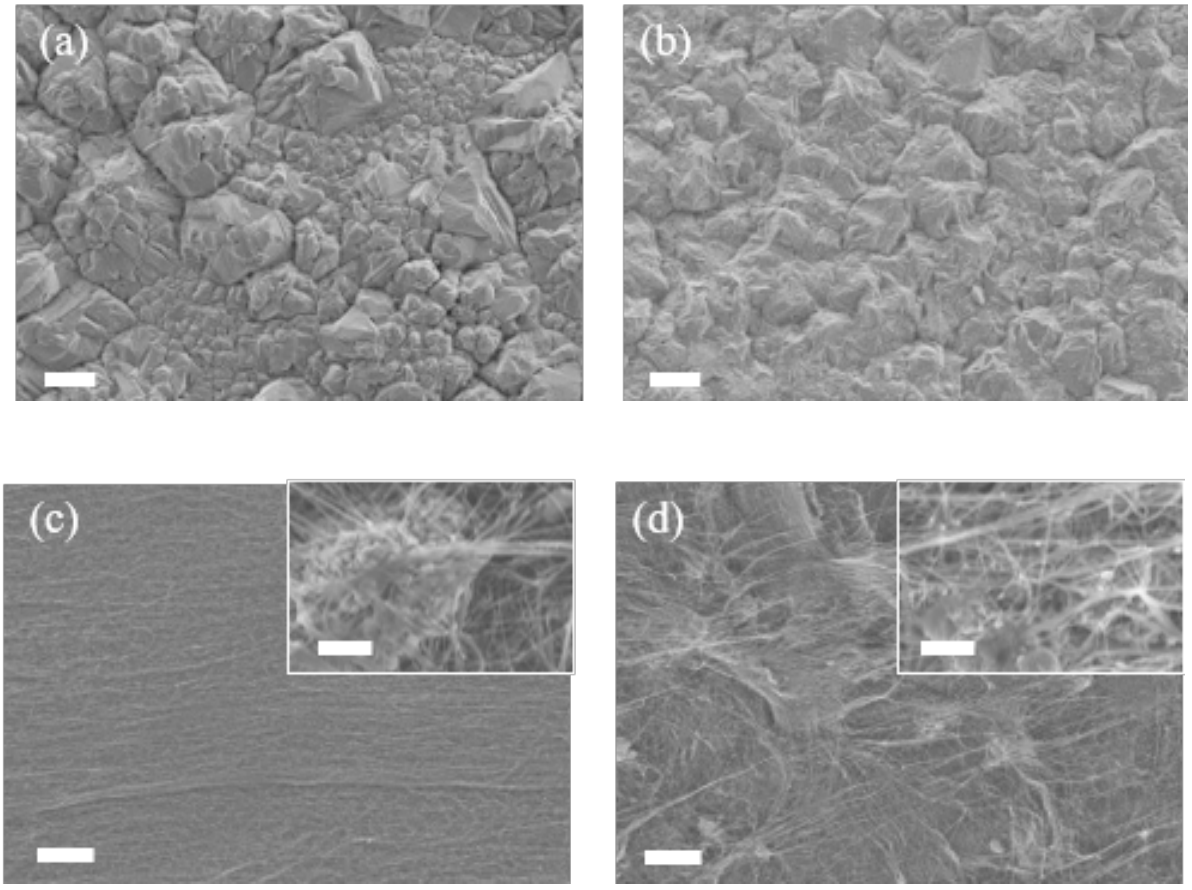

Figure 2: HR-SEM images of Cu coating deposited from $CuSO_4$ additive-free electrolytes on the CNT tissue (a, b) and inside the CNT tissue (c, d) under the following conditions:10

mA/cm^2 for 15 min.: (a, c) high Cu ion content in the electrolyte; and (b, d) low-Cu ion content in the electrolyte. Scale bar: 5 μm (inset: 500 nm).

Energy-dispersive X-ray spectroscopy (EDS) measurements obtained from the treated CNT samples (shown in **Figure S5**) indicated that the deposits comprise of only metallic Cu, and no contaminations were found on either CNT sample. This also corresponds for the metallic Cu deposited from all other electrolytes, presented and discussed in the following section. An exemplary X-ray diffraction pattern obtained from the deposits (shown in **Figure S6**) confirms their metallic nature, as well.

3.2. Cu deposition in the presence of additives in the $CuSO_4$ electrolytes

The effect of different organic additives in the $CuSO_4$ based electrolyte on Cu deposition onto and into the CNT tissues was studied. The electrolyte containing a lower Cu concentration was chosen for this part of the work, as is showed slightly higher ability to support deposition of metallic Cu inside and within the core of the CNT tissue.

3.2.1. Cu deposition in the presence of MeCN

First, the addition of acetonitrile (MeCN) to the $CuSO_4$ based electrolyte was studied. The idea to inspect the impact of MeCN originates from previous research, using an organic electrolytic bath based on MeCN for Cu deposition.[4–6,8,9] Acetonitrile (MeCN) in a concentration of 1,000 ppm was added to the electrolyte containing low Cu ions content. This concentration is within the range that has previously been found to suppress Cu nucleation without hindering its growth

rate.[14] The effect of MeCN addition on the deposition was studied. Cyclic polarization curves obtained from this electrolyte using CNT tissue and Pt working electrodes are presented in **Figure 3**a.

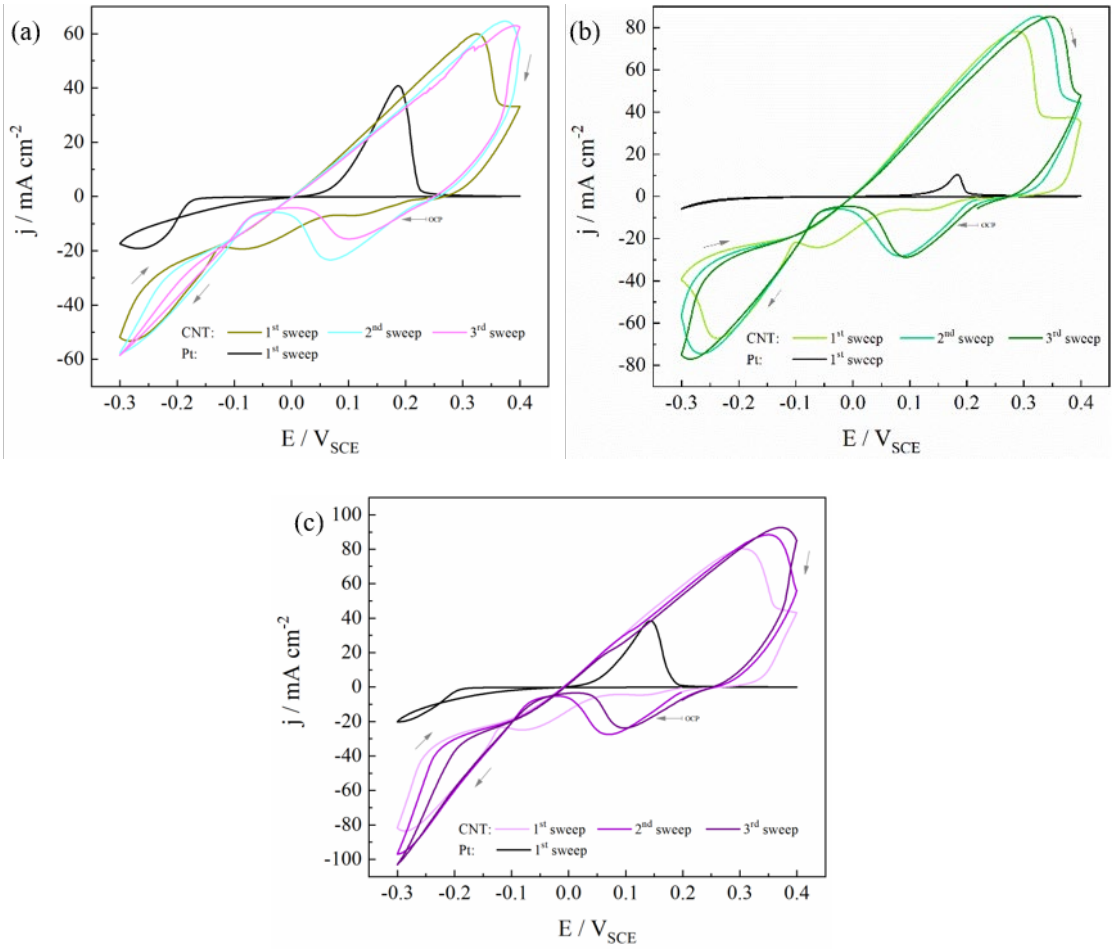

Figure 3: Cyclic polarization curves recorded with CNT working electrodes from a low-Cu ion electrolyte with various additives: (a) 1,000 ppm MeCN; (b) 500 ppm PEG; and (c) 0.1 mM BTAH.

Copper deposition on Pt electrode is inhibited once MeCN is present in the electrolyte, in respect to the additive-free electrolyte, and the nucleation overpotential stands on ca. -0.17 V_{SCE}. This is in agreement with previous findings, establishing that MeCN has an inhibition effect on Cu deposition on Pt electrodes.[14] However, the shape of the voltammograms recorded

once a CNT tissue is serving as the working electrode, resembles to the one recorded in the additive-free electrolyte, though the peaks are shifted. An increase in the cathodic currents at potentials prior to Cu deposition is observed, and the overpotential for copper nucleation stands on ca. -0.13 V_{SCE} and decreases to ca. -0.08 V_{SCE} upon further cycles. Copper deposition current is decreased upon shifting the scan direction, indicating a diffusion limitation in the system, which can be attributed to a deposition process of metallic Cu inside the CNT tissue.

3.2.3. Cu deposition in the presence of PEG

Polyethylene glycol (PEG) is a rather common additive to $CuSO_4$ based Cu plating bath electrolytes. PEG is conventionally used as a suppressing agent in the $CuSO_4$ electrolytes. The relatively large PEG molecules adsorb onto the substrate surface, alter the polarization at those specific sites, thus inhibiting the deposition on the surface. Meanwhile, due to their relatively large size, PEG molecules cannot protrude pores that are not large enough, thus deposition inside concavities, through-holes and such, is prompted. Polyethylene glycol (PEG) was added in a concentration of 500 ppm to the electrolyte containing low Cu ion concertation. This concentration is within the range of PEG concentrations, which attribute conformal copper growth [15,16]. The corresponding cyclic voltammograms were recorded for both Pt and CNT tissue, serving as working electrodes and are presented in Figure 3b. Lower deposition currents are observed once the Pt electrode is utilized as the working electrode, confirming the proclaimed inhibition effect of PEG. However, when a CNT is being used as the working electrode, we observe that Cu reduction potential is shifted toward less cathodic potentials (ca. -0.1 V_{SCE} upon first cycle, and -0.05 V_{SCE} upon consecutive sweeps). This effect is much like the one we have observed in the voltammogram obtained in the presence of MeCN additive in the electrolyte. In this case, Cu deposition is also limited by a diffusion process.

3.2.4. Cu deposition in the presence of BTAH

As known, benzotriazole (BTAH) can be used as a leveler in $CuSO_4$ electrolytes,[17] and finally it was added in a concentration of 0.1 mM to the electrolyte containing a low Cu ion content. Similar concentration of BTAH are found to have a brightening and grain-refining effect on copper coatings plated on flat electrodes.[17,18] The cyclic voltammograms recorded in this electrolyte (Figure 3c) exhibit features similar to the characteristic's features observed in the curves recorded in the presence of MeCN. Copper nucleation potential stands on ca. -0.13 V_{SCE} during the first sweep and decreases to ca. -0.07 V_{SCE} upon further sweeps. Once again, diffusion limitation is observed upon shifting the scan direction after the first vertex potential.

3.2.5. Cu deposition in the presence of additives-Morphological Studies

HR-SEM images were obtained from the CNT tissue samples after Cu deposition, both from the external coating and the inner layers of the CNT tissues (**Figure 4**). Copper coatings deposited onto the external surfaces of the CNT tissues from electrolytes containing MeCN or PEG (Figure 4a and 4b, respectively) are characterized by a lower surface coverage, in respect to Cu coatings deposited from an additive-free electrolyte (Figure 2). This indicates that Cu deposition on the outer surface is suppressed by these two organic additives. The relatively large Cu crystals deposited in the presence of MeCN (Figure 4a) may indicate that this additive blocks some of the nucleation of Cu on the outer surface of the CNT tissue. Although the surface coverage of a Cu coating deposited from an electrolyte containing BTAH achieves a higher surface coverage (Figure 4c), some gaps in the Cu coating can be observed; at these

sites a lower amount of metallic Cu has been deposited. Thus, it seems that BTAH also hinders the deposition of Cu on the external surface of the CNT tissue.

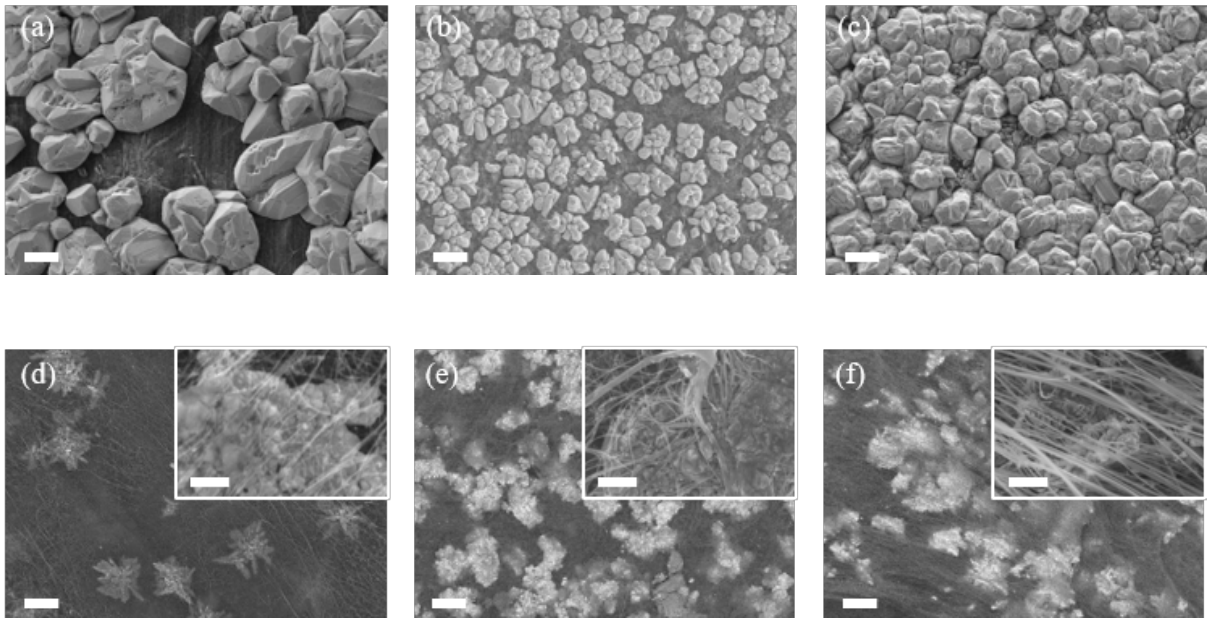

Figure 4: HR-SEM images of Cu coating deposited from a low Cu ion content in the $CuSO_4$ electrolytes on the CNT tissue surfaces (a-c) and into the core CNT tissue (d-f). (a, d) 1,000 ppm MeCN; (b, e) 500 ppm PEG; and (c, f) 0.1 mM BTAH. Electrochemical conditions: -10 mA/cm^2 for 15 min. Scale bar: 5 μm (inset: 500 nm).

Images of HR-SEM obtained from within the CNT core tissues using the ESB detector (presented in Figure 4d-f) show an increased deposition inside the CNT tissue, in the presence of all three additives, in comparison to the additive-free electrolyte (Figure 2b). Cu deposits inside the tissue (bright areas) can be clearly distinguished from the CNT matrix (darker areas) thanks to the significant difference in the atomic mass of these elements, attributing to the strong contrast in the images obtained with an ESB detector. This finding is in agreement with the cyclic voltammograms recorded in these electrolytes (Figure 3), implying deposition of Cu inside the tissue. The density of the Cu crystals inside the tissue is lower than their density on

the outer tissue surface, when deposited from the same electrolyte. Not only that, the metallic Cu crystals deposited inside the core tissue are smaller and have different morphologies than the Cu crystals deposited on the external surfaces. The Cu content deposited inside the CNT tissue from an electrolyte containing MeCN is lower than with either PEG or BTAH, perhaps as MeCN hinders the nucleation of Cu inside the tissue as well, and not only in the outer surface. The content of Cu deposited inside the CNT tissue from an electrolyte containing MeCN is lower than with either PEG or BTAH, possibly due to a non-optimal concentration of this additive in the electrolyte. Yet, it is evident that all three additives promote deposition of Cu inside the CNT tissue.

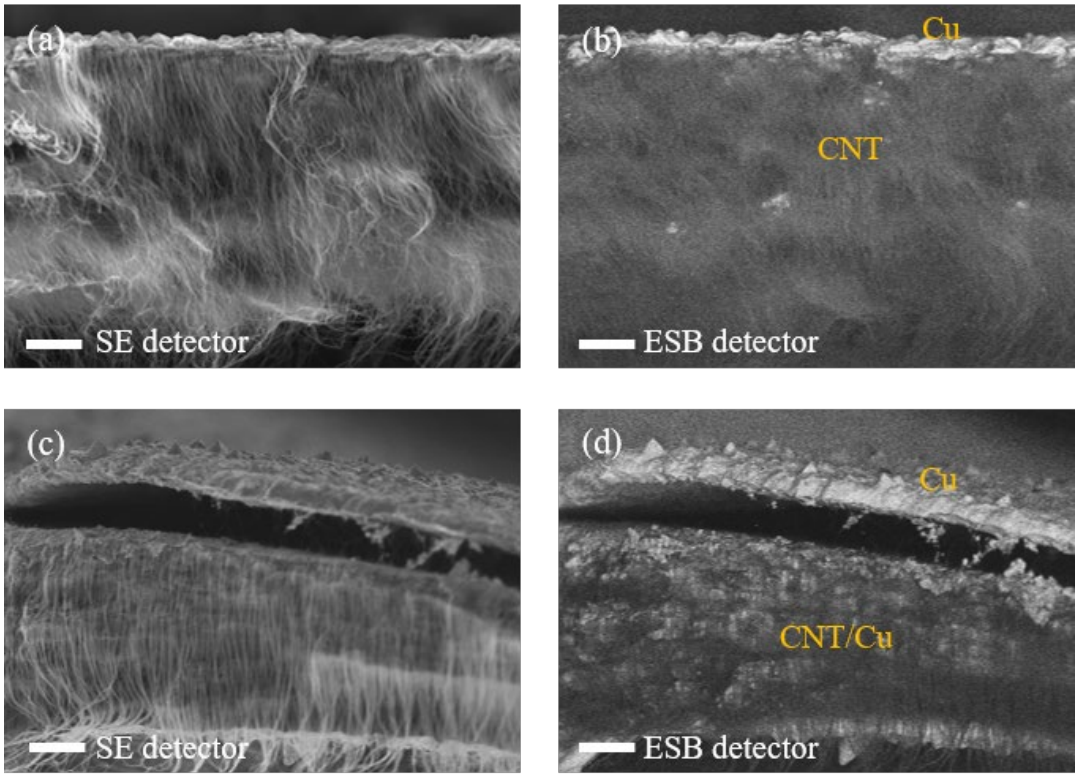

Figure 5: Cross-section HR-SEM images of Cu deposited from a low Cu ion content in the $CuSO_4$ electrolytes on the CNT tissue, from (a, b) an additive-free electrolyte; and (c-d) an

electrolyte containing 500 ppm PEG. Areas containing Cu or CNT are marked on the ESB image. Scale bar: 10 μm.

Cross-section HR-SEM images, presented in Figure 5, further corroborate these findings; when Cu deposition is carried out using an additive-free electrolyte, only an external Cu layer is formed, and no Cu is deposited inside the CNT tissue. However, when a PEG containing electrolyte is used, except for the external Cu coating, Cu crystals are also formed within the tissue, attributing to the strong contrast observed in the ESB image (Figure 5d).

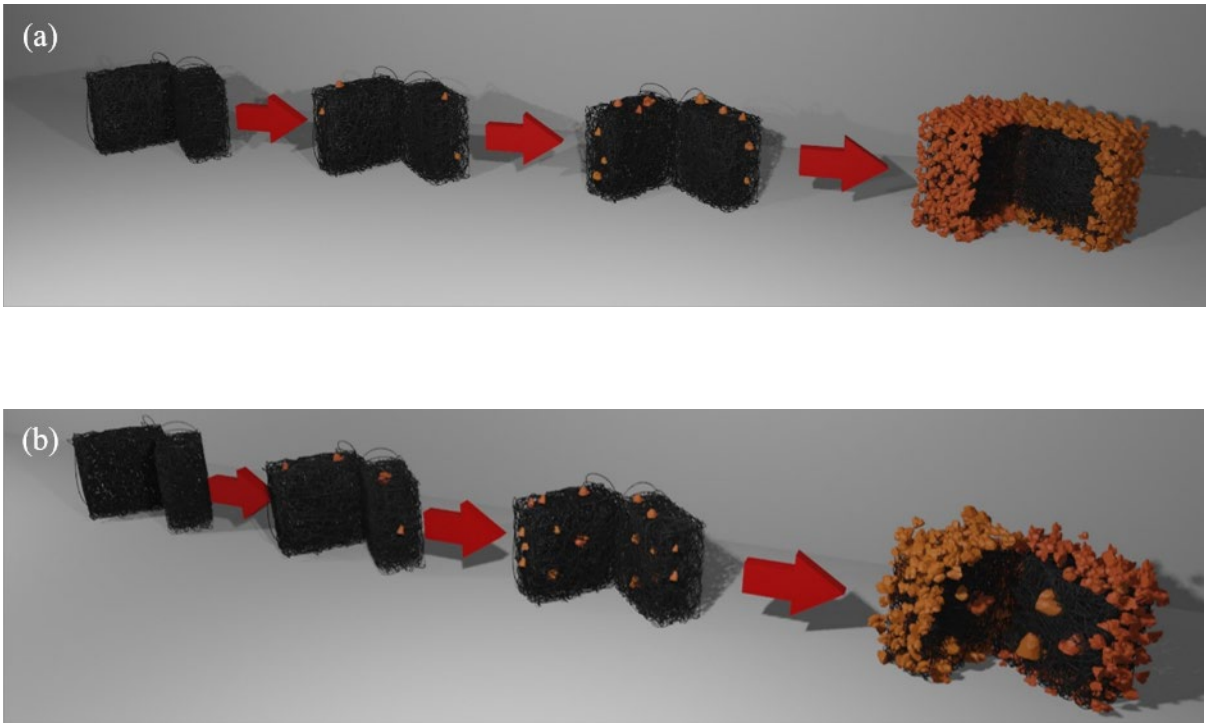

Figure 6: Schematic illustration of a CNT electrode cross-section, demonstrating the growth of Cu particles during electrodeposition from a $CuSO_4$ electrolyte: (a) without additives; (b) with organic additives, such as PEG, BTAH or MeCN.

Apparently, Cu cannot be deposited within a CNT tissue from an additive-free $CuSO_4$ electrolyte. Yet, the addition of either MeCN, PEG or BTAH does enable the deposition. Furthermore, it also decreases the extent of Cu deposition on the external surface of the CNT tissue. Thus, it appears that the three-dimensional (3D) structure of the tissue forms a barrier to the deposition inside it. The deposition on the external surface of the tissue is faster than inside it, and once the surface is fully coated, further deposition of Cu inside the tissue is highly impaired, as illustrated in Figure 6a. However, when appropriate organic additives are added, and slow the progress of surface deposition, there is more time for copper deposition inside the CNT tissue, therefore the deposition of Cu crystals is feasible using them, as depicted in Figure 6b.

4.0 Conclusions

Cu was successfully electrodeposited inside CNT tissues from multiple aqueous electrolytes. Various compositions of electrolytes based on $CuSO_4$ were developed for a single-step Cu electrodeposition inside a CNT tissue. Thus, the former claim that aqueous electrolytes are inappropriate for that task, possibly due to the CNT tissue hydrophobicity, needs to be reconsidered. The electrolytes that enable deposition inside the CNT tissue, include additives that suppress the deposition on the external surface of the electrode. An alternative explanation to the inability of the additive-free $CuSO_4$ electrolytes to enable a depositing Cu inside is suggested hereby. It is possible that Cu is not easily deposited inside the CNT tissue, despite the porosity of the tissue, because of its 3D structure. Such structure may hint that the geometric considerations are the limiting factor to an electrodeposition process inside the CNT tissue. Too low current density inside the tissue, in comparison to the outer surface, can prevent electrodeposition processes at the inner surfaces. The use of organic additives that modify the

course of deposition and hinder the deposition on the external CNT surface can thus be successfully used for this purpose.

5.0 Acknowledgements

The authors acknowledge the financial support from Israel Ministry of Energy (R&D Division, funding contract #218-11-004), the Israeli Council for Higher Education (CHE) and Israel Fuel Choice Initiative, within the framework of "Israel National Research Center for Electrochemical Propulsion" (INREP) and the Grand Technion Energy Program (GTEP). The authors also thank Ms. Katerina Bogomolov for the graphical abstract and illustrations.

6.0 References

1. G. Xu, J. Zhao, S. Li, X. Zhang, Z. Yong, and Q. Li, *Nanoscale*, **3**, 4215–4219 (2011).

2. L.K. Randeniya, A. Bendavid, P.J. Martin, and C.D. Tran, *Small*, **6**, 1806–1811 (2010).

3. J. Shuai, L. Xiong, L. Zhu, and W. Li, *Compos. Part A*, **88**, 148–155 (2016).

4. C. Subramaniam, T. Yamada, K. Kobashi, A. Sekiguchi, D.N. Futaba, M. Yumura and K. Hata, *Nat. Commun.*, **4**, 1–7 (2013) http://dx.doi.org/10.1038/ncomms3202.

5. R. Sundaram, T. Yamada, K. Hata, and A. Sekiguchi, *Mater. Today Commun.*, **13**, 119–125 (2017).

6. C. Subramaniam, A. Sekiguchi, T. Yamada, D. N. Futaba, and K. Hata, *Nanoscale*, **8**, 3888–3894 (2016).

7. C. Subramaniam, Y. Yasuda, S. Takeya, S. Ata, A. Nishizawa, D. Futaba, A.

Nishizawa, D. Futaba, T. Yamada and K. Hata, *Nanoscale*, **6**, 2669–2674 (2014).

8. R. Sundaram, T. Yamada, K. Hata, and A. Sekiguchi, *Sci. Rep.*, **7**, 1–11 (2017).

9. R. Sundaram, T. Yamada, K. Hata, and A. Sekiguchi, *Jpn. J. Appl. Phys.*, **57**, 04FP08 (2018).

10. M. Schlesinger and M. Paunovic, *Modern Electroplating*, 5th Ed., p. 1-737, John Wiley & Sons, Inc., (2010).

11. P. Puech, T. Spalkin, A. Gerber, V. Tishkova, E. Pavlenko, …and W. Bacsa, *Phys. Rev. B*, **85**, 205412 (2012).

12. N.N.C. Isa, Y. Mohd, M.H.M. Zaki, and S.A.S. Mohamad, *Int. J. Electrochem. Sci.*, **12**, 6010–6021 (2017).

13. D. M. Kabtamu G.-Y. Lin, Y.-C. Chang, H.-Y. Chen, H.-C. Huang, N.-Y. Hsu, Y.-S. Chou, H.-J. Wei and C.-H. Wang, *RSC Adv.*, **8**, 8537–8543 (2018).

14. A.V. Rudnev, E.B. Molodkina, A.I. Danilov, Y.M. Polukarov, and J.M. Feliu, *Russ. J. Electrochem.*, **42**, 381–392 (2006).

15. K. Kondo, R.N. Akolkar, D.P. Barkey, and M. Yokoi, *Copper Electrodeposition for Nanofabrication of Electronics Devices*, p. 282, Springer Science, (2014).

16. L. Yin, Z.H. Liu, Z.P. Yang, Z.L. Wang, and S. Shingubara, *Trans. Inst. Met. Finish.*, **88**, 149–153 (2010).

17. N. Tantavichet and M. Pritzker, *J. Appl. Electrochem.*, **36**, 49–61 (2006).

18. T.Y.B. Leung, M. Kang, B.F. Corry, and A.A. Gewirth, *J. Electrochem. Soc.*, **147**, 3326–3337 (2000).

Figure Captions:

Figure 7: Cyclic polarization curves recorded with CNT working electrodes from additive-free $CuSO_4$ electrolytes: (a) high-Cu ion content in the electrolyte; (b), (c) low-Cu ion content in the electrolyte.

Figure 8: HR-SEM images of Cu coating deposited from $CuSO_4$ additive-free electrolytes on the CNT tissue (a, b) and inside the CNT tissue (c, d) under the following conditions:10 mA/cm^2 for 15 min.: (a, c) high Cu ion content in the electrolyte; and (b, d) low-Cu ion content in the electrolyte. Scale bar: 5 μm (inset: 500 nm).

Figure 9: Cyclic polarization curves recorded with CNT working electrodes from a low-Cu ion electrolyte with various additives: (a) 1,000 ppm MeCN; (b) 500 ppm PEG; and (c) 0.1 mM BTAH.

Figure 10: HR-SEM images of Cu coating deposited from a low Cu ion content in the $CuSO_4$ electrolytes on the CNT tissue surfaces (a-c) and into the core CNT tissue (d-f). (a, d) 1,000 ppm MeCN; (b, e) 500 ppm PEG; and (c, f) 0.1 mM BTAH. Electrochemical conditions: -10 mA/cm^2 for 15 min. Scale bar: 5 μm (inset: 500 nm).

Figure 11: Cross-section HR-SEM images of Cu deposited from a low Cu ion content in the $CuSO_4$ electrolytes on the CNT tissue, from (a, b) an additive-free electrolyte; and (c-d) an electrolyte containing 500 ppm PEG. Areas containing Cu or CNT are marked on the ESB image. Scale bar: 10 μm.

Figure 12: Schematic illustration of a CNT electrode cross-section, demonstrating the growth of Cu particles during electrodeposition from a $CuSO_4$ electrolyte: (a) without additives; (b) with organic additives, such as PEG, BTAH or MeCN.